45th AIAA/ASME/ASCE/AHS/ASC Structures, Structural Dynamics & Materials Conference
19 - 22 April 2004, Palm Springs, California

AIAA 2004-1924

SELECTIVE REINFORCEMENT TO IMPROVE FRACTURE TOUGHNESS AND FATIGUE CRACK GROWTH RESISTANCE IN METALLIC STRUCTURES

Gary L. Farley[*] and John A. Newman[†]
Army Research Laboratory
Vehicle Technology Directorate
Langley Research Center
Hampton, VA 23681
Gary.L.Farley@NASA.Gov
John.A.Newman@NASA.Gov

Mark A. James[‡]
National Institute for Aerospace
Langley Research Center
Hampton, VA 23681
(757) 864-3457
james@nianet.org

ABSTRACT

Experimental and analytical investigations of the fatigue crack growth and fracture response of aluminum selectively reinforced compact tension specimens were performed. It was shown that selective reinforcement significantly improved these responses primarily through load sharing by the reinforcement. With the appropriate combination of reinforcement architecture and mechanical properties, as well as reinforcement to base aluminum interface properties, fatigue cracks can be arrested using selective reinforcement. Maximum load associated with fracture increased up to 20 percent for the cases investigated and crack growth at maximum load increased as much as 150 percent. For both fatigue crack growth and fracture, the three most influential properties identified within the bounds of this investigation that influence this response are reinforcement width, reinforcement stiffness and interface stiffness. Considerable coupling occurs between the different fiber architecture and material properties and how they influence fatigue crack growth and fracture responses.

---

[*] Non-AIAA member, Aerospace Engineer, Mechanics and Durability Branch.
[†] Non-AIAA member, Aerospace Engineer, Mechanics and Durability Branch.
[‡] Non-AIAA member, Resident Researcher, NIA, Mechanics and Durability Branch.

INTRODUCTION

Aluminum alloys have been a mainstay structural material for aerospace, marine, automotive and sports equipment applications for more than one half a century and are considered the performance and fabrication cost benchmark for new materials. New aluminum alloys and fabrication technologies maintain this prominence by providing enhanced mechanical properties and reduced cost. Although the overall performance of aluminum alloys continues to improve, tradeoffs among corrosion, fatigue crack growth resistance, fracture toughness, stiffness and strength can at times justify considering other materials.

Selective reinforcement is a structural design concept where small quantities of reinforcement, nominally less than 5 percent by weight of the component, is intelligently applied to locally tailor stiffness and strength, thus enhancing structural performance and / or reducing weight.[1] Specific buckling and post-buckling performance of selectively reinforced aluminum panels can exceed the performance of geometrically comparable unreinforced aluminum panels by as much as 60 percent.[1] The specific performance of reinforced metallic panels can surpass the performance of geometrically comparable polymer matrix composite panels.[1]

Selective reinforcements may be applied in ribbon like form near the surface of the base aluminum structure, as depicted in Figure 1, to increase inplane and bending stiffness.[1] One is compelled to question whether these reinforcements have other structural attributes, such as enhanced fatigue crack growth resistance and increased fracture toughness of the overall structure. Any fatigue crack growth or fracture benefits may be without weight or cost penalty if the reinforcement was originally applied to enhance other performance characteristics, such as buckling or post-buckling response.

The objective of this experimental and analytical investigation is to determine the effects of selective reinforcement on fatigue crack growth driving force and fracture toughness of aluminum. Fatigue crack growth and fracture tests are conducted and the results assessed for unreinforced and selectively reinforced aluminum compact tension specimens. Parametric analytical studies are conducted on unreinforced and selectively reinforced compact tension specimens to investigate how reinforcement geometry and material properties affect fatigue crack growth and fracture response.
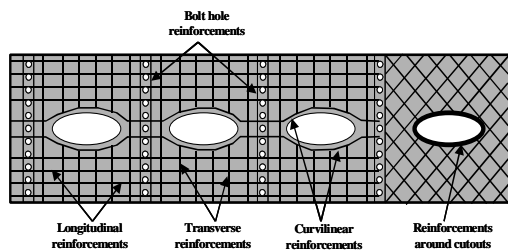

Figure 1. Depiction of a wing skin with multiple selective reinforcement architectures across the skin, around cutouts and along fastener rows.

EXPERIMENT

This section describes the test specimens, materials and test procedures used in this study. Both the fatigue crack growth and fracture toughness tests utilized identical geometry compact tension specimens. Unreinforced aluminum compact tension specimens are included to provide a baseline for comparison.

Compact Tension Specimens

The compact tension (CT) specimen, as shown in Figure 2, was used in both the fatigue crack growth and fracture studies.[2] Specimens had width and thickness dimensions of 2.4 inch and 0.10 inch, respectively, and were made of aluminum alloy 7075. Reinforced specimens had two slots per side, 0.50" wide and 0.02" deep, machined in the loading direction, as shown in Figure 2. Distance between reinforcements was 0.50". A ribbon of continuous reinforcement, consisting of 40 percent volume fraction of alumina oxide (Al_2O_3) fibers embedded in an aluminum matrix (alloy 1100) was embedded into each slot and bonded with a commercial structural epoxy adhesive. Glass micro-spheres 0.003" in diameter were added to the adhesive (less than 1 percent by volume) to maintain bond line thickness. Bond surface preparation and curing procedures as per adhesive manufacturers recommendations were followed. The width of the reinforcement ribbons was approximately 0.50" and had a thickness of approximately 0.017".
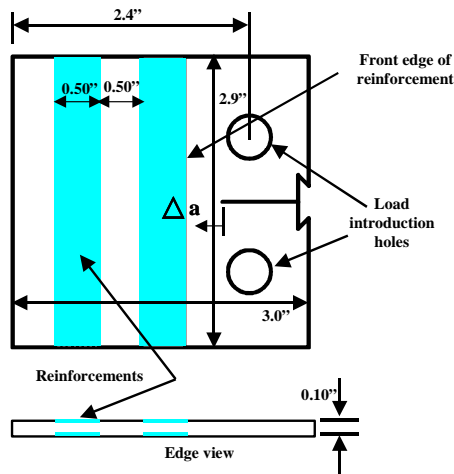
American Institute of Aeronautics and Astronautics

Figure 2. Reinforced compact tension specimen.

Test Procedures

Both fatigue and fracture test specimens were subjected to a tension-tension fatigue loading pre-cracking procedure. The maximum tension force was 300 lb$_f$ with a load ratio (R) of 0.1 cyclically loaded at 10Hz. Approximately 30K cycles were required to initiate a fatigue crack with approximately 0.03" of crack growth from the crack starter notch. Both the front and backsides of the CT specimens were polished to facilitate tracking the crack tip. A microscope attached to a digital caliper base mounted to the test machine was used to measure crack length during tests.

Fatigue crack growth tests were performed under the same load conditions used for pre-cracking {maximum load (P$_{max}$) = 300 lb$_f$, R = 0.1, cyclically loaded at 10 Hz}. Tests were periodically halted to visually measure the crack tip location. The crack tip was not visible when the crack traversed beneath the reinforcement, so after the crack reached the reinforcement the fatigue test was allowed to run non-stop until a prescribed number of load cycles was completed. Final crack tip location was determined by destructively sectioning the specimen at the leading edge of the reinforcement and then progressively grinding and polishing the specimen surface to determine the crack tip location.

The fatigue crack growth tests consisted of one baseline unreinforced and two reinforced specimens. Approximately 80K fatigue cycles were applied to the unreinforced specimen while 200K and 500K fatigue cycles were applied to the reinforced specimens.

Quasi-static displacement-controlled fracture tests were performed on both baseline unreinforced and reinforced specimens. During these tests test machine head displacement was slowly increased until the crack propagated. For each crack growth increment the maximum load, test machine head displacement, and total crack growth were recorded. This procedure was successively applied throughout the test. Specimen crack growth was measured in a similar manner as in the fatigue crack growth tests.

ANALYSIS

The Fracture Analysis Code Two-Dimensional Layered (FRANC2DL) finite element computer program[3,4] was used to parametrically study both fatigue crack growth and fracture toughness of selectively reinforced CT specimens. The computer program FRANC2DL is designed for the simulation of crack growth in a layered structure. Linear elastic fracture mechanics was used to simulate fatigue crack growth and elastic-plastic tearing was used to simulate fracture. These procedures are described in detail in the following sections.

Fatigue Crack Growth Analysis

The finite element model, depicted in Figure 3, for the reinforced compact tension specimen consisted of three two-dimensional layers: upper and lower reinforcement layers and a middle base aluminum layer. Identical finite element meshes were used in the reinforcement layers. These meshes coincided with the base layer mesh in the reinforcement region. Reinforcement layers were mathematically linked to the base aluminum layer using adhesive (interface) elements. This linkage between the base aluminum and the reinforcement is referred to as an interface, and the influence of interface thickness and material stiffness was separated in this study. In the reinforced model, the thickness of the middle aluminum layer beneath the reinforcements was reduced by the total thickness of the reinforcements. The model for the unreinforced specimen consisted of just the aluminum layer with a constant thickness. Within this parametric study, reinforcement width was a variable; therefore individual finite element models were developed for each reinforcement width

evaluated. In all cases the location of the front edge of the reinforcement, as defined in Figure 2, was held constant with respect to the centerline of the load introduction holes.
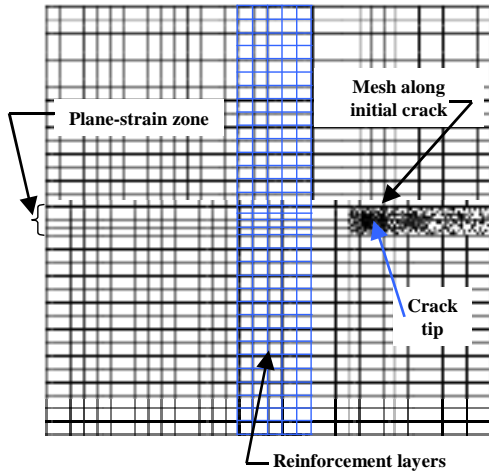

Figure 3. Finite element model of compact tension specimen used in fatigue crack growth analyses.

Although the reinforced test specimens had two reinforcements per side it was determined during preliminary analysis that a model containing just one, the first reinforcement, produced the same fatigue crack growth results as a model containing two reinforcements. Therefore, to reduce the total number of degrees of freedom in the model and expedite computational times, all reported fatigue analyses were based upon a model having a single reinforcement per side. Also, the thickness of the aluminum where the second reinforcement would have been located was modeled as the same thickness as the aluminum away from the reinforcements.

The finite element model consisted of two-dimensional, eight-node-quadrilateral, membrane finite elements. When the crack was initiated and subsequently propagated, the computer program utilized an automatic re-meshing scheme with six node triangular membrane finite elements. As the crack propagated, the number of elements and subsequent degrees of freedom increased. At the beginning of the analysis there were approximately 10,000 degrees of freedom within a model. At the end of an analysis after crack extension and re-meshing the number of degrees of freedom in the model doubled.

The material mechanical properties used in these analyses are listed in Table 1. Material properties for reinforcement materials that had other than 50 percent fiber volume fraction was adjusted based upon the rule of mixture.

Material	E_{11} (Msi)	E_{22} (Msi)	G_{12} (Msi)	ν_{12}	Strength (Ksi)
7075 Aluminum	10.0	10.0	3.84	0.3	72.5
Alumina oxide reinforced aluminum	35.0	19.0	6.72	0.25	250.0

Table 1. Material properties used in finite element analyses.

The fatigue crack growth analyses could be accurately simulated as a series of linear analyses using linear elastic fracture mechanics. This allowed a unit load to be applied to the model for each crack tip location. The stress-intensity factor was calculated and recorded for each location. For crack growth, a new crack tip location was manually defined and the computer program subsequently re-meshed the model automatically. Using this method, all models with the same geometry had an identical finite element mesh after each increment in crack length.

After the unit load was applied to the specimen, the stress intensity factor was calculated. A normalized stress intensity factor was calculated using the unit load stress intensity factor multiplied by the magnitude of the experimental fatigue load delta (300 lb$_f$ - 30 lb$_f$ = 270 lb$_f$) and divided by the stress intensity threshold (the stress intensity factor below which no crack growth occurs, 2 ksi-in$^{1/2}$ for a 0.10" thick 7075 aluminum). A normalized stress-intensity factor less than one means crack growth will not occur. The normalized stress-intensity factor as a function of crack growth was recorded and subsequently plotted. Reinforcement failure was not modeled for the fatigue crack growth studies because fatigue-loading levels for fatigue crack growth are well below those that would lead to reinforcement failure.

The first part of this study was the validation of the analysis by comparing predicted fatigue crack growth with experimental results for the reinforced specimens. A parametric analytical investigation was then conducted on the effects of reinforcement width, reinforcement thickness, reinforcement stiffness, interface stiffness, and interface thickness. All results were compared to the unreinforced baseline results. Three reinforcement

widths were investigated (0.50", 0.25" and 0.10"). Reinforcement thickness on each surface was either 0.02" or 0.04" corresponding to 40 and 80 percent, respectively, of the thickness of the total specimen. The effect of reinforcement stiffness was calculated by varying reinforcement fiber volume fraction (50, 30, and 10 percent). Interface stiffness was varied to approximate two methods (adhesive bond or weld) for attaching the reinforcement to the base aluminum. The flexible interface (adhesive bond) had a shear stiffness (G) of 0.1 Msi and the stiff interface (weld) had shear stiffness equal to the wrought aluminum material (3.84Msi). These cases are assumed to be two extremes and it is reasonable to expect all other reinforcement bonding techniques to fall within this range. Interface thickness effects were investigated by analyzing specimens having thicknesses of 0.001", 0.005" and 0.010".

Fracture Analysis

An elastic-plastic tearing analysis was performed to simulate the fracture process for unreinforced and reinforced compact tension specimens. Finite element models were developed to take advantage of the symmetry about the initial crack plane. Reinforced specimens were modeled using layers in a manner similar to the fatigue crack growth analysis. To adequately represent the three-dimensional deformation state in the vicinity of the crack tip using two-dimensional elements requires the use of plain-strain finite elements.[5,6] A band of plane-strain finite elements was located within a region equal to the thickness of the specimen and along the crack path. [5,6] All finite elements outside of this region and within the reinforcements were modeled as plane-stress elements. All finite elements were assumed to exhibit small strain material nonlinearity using an elastic-perfectly plastic von Mises model, except those in the reinforcement and in the vicinity where the load introduction pin is located, which were modeled as linear elastic. It was necessary to model the elements around the load introduction point as linear elastic to simulate, without geometrically modeling, load transfer from the load introduction pin into the specimen without creating local material yielding.

The aluminum base material was assumed to be elastic perfectly plastic with a yield stress of 72.5 ksi, the yield stress of 7075 aluminum. The same elastic material mechanical properties for the aluminum and reinforcement material as used in

the fatigue crack growth analyses were used in these analyses. The tearing analyses used the constant crack tip opening displacement (CTOD) fracture criterion. This criterion, measured 0.04" behind the moving crack tip, is equivalent to the crack tip opening angle criterion.[5,6] Multi-point constraints along the specimen symmetry plane were sequentially released along the crack path to simulate crack growth.

An analysis of both unreinforced and reinforced specimens was performed and the results compared with experimental results to validate the analysis. In the reinforced specimen, failure of the reinforcement was assumed when the inplane stress parallel to the fiber direction exceeded the reinforcement material strength. Progressive interface layer failure was not incorporated in the parametric study based upon a preliminary analysis showing it had a negligible effect on the predicted reinforcement failure load.

Parametric studies investigating the effect of reinforcement width and thickness, and interface stiffness were conducted. Reinforcement widths investigated were 1.00", 0.50" and 0.25". Reinforcement thickness on each side of the specimen was either 0.02" or 0.04" resulting in reinforcement thickness as a percent of total thickness of 40 and 80 percent, respectively. The effect of interface stiffness was investigated using the same shear moduli values used in the fatigue crack growth analysis (0.1 and 3.84 Msi).

RESULTS AND DISCUSSION

The experimental and analytical results from the fatigue crack growth study will be presented first followed by the experimental and analytical results from the fracture study. Within each of these studies the experimental results are presented first followed by the validation analysis and then the results from the analytical parametric study.

Experimental Fatigue Crack Growth

The experimental fatigue crack growth results are presented in Figure 4. Data for the unreinforced specimen is shown as a nonlinear curve (blue diamond symbols) such that the slope of the curve, which is the crack growth rate, increases with increasing crack growth. This increase in crack growth rate occurs because the crack driving force increase with crack length during constant-load testing. Testing of the unreinforced specimen was

stopped at approximately 80K cycles, as specimen failure was imminent. No additional testing was performed on unreinforced material.

The results of two different fatigue crack growth tests performed on reinforced specimens are plotted in Figure 4 and are seen to be in good agreement (less than 5 percent difference between data sets). For the reinforced material the crack propagated under the leading edge of the reinforcement at approximately 100K cycles, approximately a 30 percent improvement, compared to the unreinforced specimens, in crack growth life to a crack size of nearly 0.38 inch. To this point in the tests, the crack growth data for all tests showed positive crack growth rates (slope) with increasing crack length. Based on the results of the unreinforced material, failure of the reinforced material would therefore be expected to occur at approximately 110K cycles, if trends were to continue. Testing of the reinforced specimens were stopped at 200K and 500K fatigue cycles with no fatigue crack propagation beyond the trailing edge of the reinforcement. The destructive crack length data are shown as the two symbols between the horizontal dashed lines. The dotted curve is shown connecting these two data points with the rest of the data set to show the likely crack length versus cycle behavior.
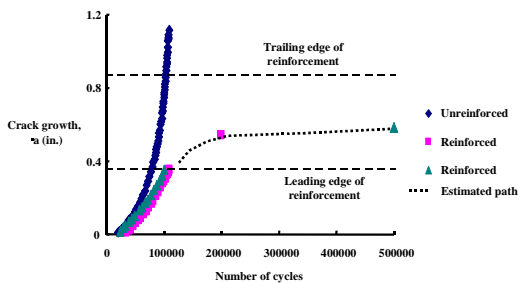

Figure 4. Experimental fatigue crack growth results.

The differences in crack lengths of the specimens tested at 200K and 500K cycles are within the data scatter between specimens observed prior to the crack tip extending beneath the reinforcement. Therefore, it cannot be determined if crack arrest or just sever crack retardation occurred as the crack grew under the reinforced material. Regardless, these data show a significant improvement in crack growth resistance, at least for the load levels considered.

Analytical Fatigue Crack Growth

In order to assess the ability to predict fatigue crack growth, an analysis was performed of a specimen having a 0.50" wide reinforcement and the crack arrested beneath the reinforcement at approximately 0.16" from the reinforcement's leading edge. From the experimental results depicted in Figure 4, the crack tip extended beneath the reinforcement between 0.15" and 0.18" from the leading edge. The agreement between analysis and test is considered good and provides confidence in using the FRANC2DL computer program for this parametric study.

A parametric analytical investigation of the influence of reinforcement geometry, reinforcement stiffness and interface stiffness on fatigue crack growth was conducted and the results are presented in Figures 5 thru 9. Unless otherwise noted, all specimens have a flexible interface between the reinforcement and base aluminum. The results are presented in terms of stress-intensity factor (also referred to as crack driving force) normalized by the threshold stress-intensity factor as a function of crack length. A normalized stress intensity factor less than 1 means no crack growth occurs. No determination of whether the reinforcement has failed at a prescribed crack length was made for the fatigue crack growth study. The predicted response of the unreinforced specimen is included for comparison purpose. Small undulations in the otherwise smooth response curves, in particular for the unreinforced specimen, are due to poor mesh geometry at a particular crack tip position. These small undulations do not adversely affect the data trends.

The effect of reinforcement width on fatigue crack growth response is depicted in Figure 5. For the reinforcement geometries, specimen dimension and material properties selected for this case, only the 0.50" wide reinforcement will arrest the fatigue crack. In this case the crack grows approximately 0.15" past the leading edge of the reinforcement. Crack growth response for the specimen having a 0.25" wide reinforcement almost reaches the no-growth state before the crack reaches the trailing edge of the reinforcement, whereas the specimen having a 0.10" wide reinforcement never achieves the no-crack growth state.

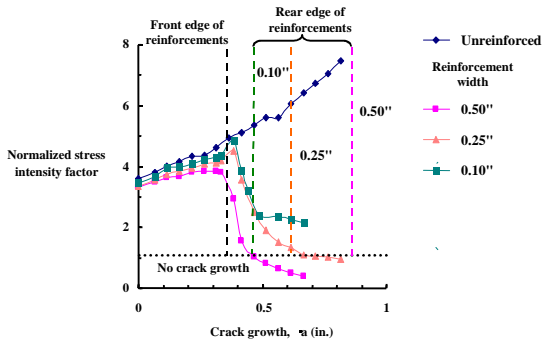American Institute of Aeronautics and Astronautics

Figure 5. Predicted effect of reinforcement width on fatigue crack growth (flexible interface, reinforcement thickness = 40 percent).

Specimens having reinforcement 0.10" or 0.50" wide and reinforcement extending 40 percent through the thickness were evaluated for two distinct interface stiffnesses. As depicted in Figure 6, the crack in the specimen with the flexible interface (polymer based adhesive) and a width of 0.10" will not achieve the no-growth state. However, for the specimen having the same reinforcement width and having interface stiffness on the order of the stiffness of the base material, a no-growth state was obtained after only a slight extension beneath the reinforcement. For this combination of reinforcement geometry, material properties and loading conditions, interface stiffness had a significant affect on fatigue crack growth response, but for other specimen configurations, such as the 0.50" wide reinforcement, the affect was less significant. Furthermore, specimens having 0.10" and 0.50" reinforcements with a stiff interface had nearly equal crack growth response at the no-growth state
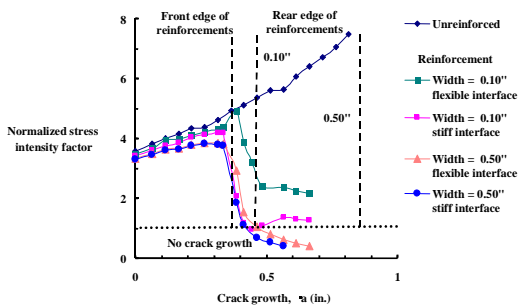

Figure 6. Predicted effect of interface stiffness on fatigue crack growth (reinforcement thickness = 40 percent).

indicating that the stiff interface significantly increased the effectiveness of load transfer to the reinforcement. Furthermore, as the interface stiffness increased, load was transferred to the reinforcement when the crack tip was further away from the reinforcement.

The effect of reinforcement thickness on fatigue crack growth is presented in Figure 7 for specimens having reinforcement width of 0.25" with reinforcement thickness 40 or 80 percent of the total thickness. All specimens had a flexible interface. As reinforcement thickness increased the no-growth state was achieved at a lower crack length indicating that additional load was carried by the increased reinforcement thickness.

The fatigue crack growth response exhibits considerable coupling between reinforcement width and thickness, base material thickness and interface stiffness. For instance the stiffness of a reinforcement that is 0.25" wide and whose total thickness is 80 percent is equal to that of a reinforcement that is 0.50" wide and having a total thickness of 40 percent. However, the responses are not the same. The 0.50" reinforcement reaches a no-crack growth state at approximately 0.45" whereas the 0.25" reinforcement reached a no-crack growth state at approximately 0.60". Two important differences between these specimens are the thickness of the base aluminum beneath the reinforcement and the width of the reinforcement. In the case of the 0.50" wide reinforcement, the base aluminum was three times thicker and twice as wide as the 0.25" wide reinforcement. The thicker base aluminum requires a higher P_{max} to achieve the same crack growth as achieved in a thinner specimen and therefore a shorter crack growth occurred for the wider reinforced specimen that had a thinner reinforcement.

The effect of reinforcement stiffness on fatigue crack growth was investigated by analytically varying the fiber volume fraction within the reinforcement. Three fiber volume fractions (50, 30 and 10 percent) were evaluated for 0.5" wide reinforcements with the reinforcement consisting of 40 percent of the total thickness and having a flexible interface. As depicted in Figure 8, as fiber volume fraction increased (hence as stiffness increases) the crack growth to reach a no-growth state decreased.

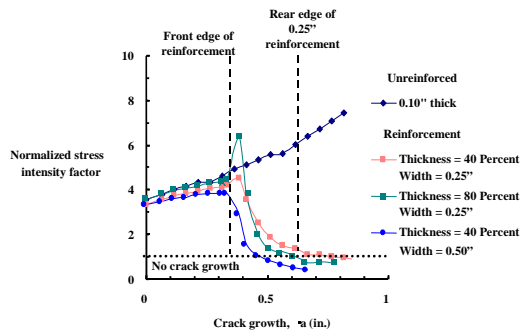American Institute of Aeronautics and Astronautics

Figure 7. Predicted effect of reinforcement thickness, as a percentage of total thickness, on fatigue crack growth (flexible interface).

Interface layer thickness is another parameter that influences the load transfer between the base aluminum and the reinforcement. A specimen with 0.5" wide reinforcement was analyzed using a flexible interface. Three interface layer thicknesses (0.001", 0.005", and 0.010") were investigated to determine their affect on crack growth. As depicted in Figure 9, the thinner the interface layer the shorter the crack growth before a no-growth state was reached.
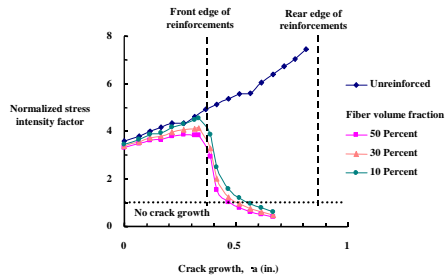

Figure 8. Predicted effect of reinforcement stiffness on fatigue crack growth (reinforcement width = 0.5", reinforcement thickness = 40 percent, flexible interface).

The aforementioned parametric studies provide sufficient information to create a reasonable description of the cause-effect relationship for the fatigue crack growth response in selectively reinforced materials. Reinforcement affects fatigue crack growth through load sharing. That is, if the reinforcement can react a sufficient portion of the load such that the stress-intensity factor in the base material is below the local threshold stress-intensity factor, then crack growth will stop.
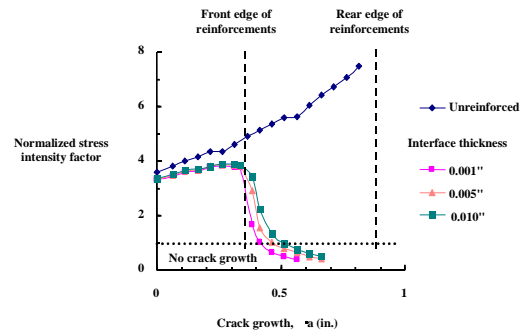

Figure 9. Predicted effect of interface thickness on fatigue crack growth (reinforcement width = 0.5", reinforcement thickness = 40 percent, flexible interface).

More specifically, when the fatigue crack tip is multiple specimen thicknesses from the reinforcement the reinforcement reacts a small portion of the applied load and the load in the reinforcement is generally compressive. Based upon examination of stress contours, not shown herein, as the crack tip grew toward the reinforcement, load in the reinforcement changed from compression to tension between one and three specimen thickness from the edge of the reinforcement. The flexibility of the interface layer, that is the combined effect of the shear stiffness and thickness, controls load transfer to the reinforcement. The more flexible the interface, that is the lower the shear stiffness or the thicker the interface, the less effective is the load transfer and the longer the crack must grow before significant load is transferred to the reinforcement. As the crack further extends toward and eventually extends beneath the reinforcement, more tensile load is reacted by the reinforcement and the stress state in the reinforcement becomes concentrated at the crack tip. For those combinations of reinforcement geometry, reinforcement stiffness and interface stiffness where the stress-intensity factor in the base aluminum beneath the reinforcement decreases below the local threshold value then crack growth stops. However, parametric studies showed that there are combinations of reinforcement geometry, reinforcement stiffness, and interface stiffness that do not create sufficient load sharing capability in the reinforcement to reduce the stress-intensity factor below the threshold value.

An interesting characteristic of the response curve is the increase in normalized stress intensity factor as the crack tip extends beyond the leading edge of the stiffener, creating a "hump" in the response curve such as depicted in Figures 5 thru 7. A "hump" in the response curve is a coupling of many parameters that ultimately produce this response. For instance, thickness reduction in the base aluminum, as a result of a thicker reinforcement, causes an increase in local threshold stress-intensity factor in the base aluminum, hence an increase in the normalized stress-intensity factor, such as depicted in Figure 7 for the specimen that has a 0.25" wide reinforcement with 80 percent through-the-thickness reinforcement. As crack growth progresses beneath the reinforcement, the reinforcement reacts a larger percentage of the load from the base aluminum. The load transfer to the reinforcement results in a significant decrease in the stress-intensity factor causing a significant change in slope of the response curve. Furthermore, the magnitude of the slope of the response curve increases, that is it has an increasing negative slope, as an increasing amount of load is transferred from the base aluminum to the reinforcement.

A narrow reinforcement allows the crack to propagate further beneath the reinforcement before sufficient load is shared to achieve a no-growth state. When the crack progresses beneath the reinforcement the effect of reduced base aluminum thickness results in an increase in the local threshold stress intensity factor as previously described for the case of the effect of increasing reinforcement thickness. Higher interface stiffness reduces the magnitude of the "hump". When the interface stiffness reaches the wrought base aluminum properties then the "hump" behavior is minimized because the reinforcement begins significantly contributing in the load sharing before the crack tip reaches the edge of the reinforcement.

Experimental Fracture Toughness

The experimental fracture toughness test results are presented in Figure 10 as applied load versus measured crack growth. Load as a function of crack growth for the unreinforced specimen exhibited a saw tooth response curve due to a succession of incremental small crack growth steps resulting from stable tearing followed by larger dynamic events. The overall response of the
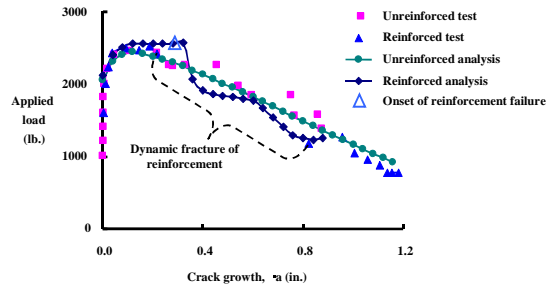

Figure 10. Experiment and predicted fracture response of unreinforced and reinforced specimens.

reinforced specimen was similar except when the reinforcement failed the crack dynamically extended across the reinforcement. Although the general trends were similar there are differences. The reinforced specimen exhibited a slight increase in toughness, which is attributed to the load sharing created by the reinforcement. The reinforced specimen's response curve flattens at the peak region relative to the more rounded response of the unreinforced specimen. It was observed that reinforcement failure occurred when the crack grew to the leading edge of the reinforcement. Just prior to reinforcement failure the load was higher than recorded at the previous step, although an exact data value was not recorded due to the dynamic nature of the reinforcement failure. The approximate load and crack length prior to reinforcement failure is identified in Figure 10 by an open triangular symbol. Maximum load occurs when as the crack reaches the leading edge of the reinforcement. Crack length at maximum load increased approximately 150 percent relative to the unreinforced specimen. Increasing crack length prior to reaching maximum load is important from an inspection perspective because the crack becomes more readily detectable.

Analytical Fracture Toughness

To validate the analysis for the parametric study, an elastic-plastic analysis was performed for both the unreinforced and reinforced specimens and the results presented in Figure 10. Crack tip advancement was based upon the computed crack tip opening displacement (CTOD). Critical value of CTOD was determined by matching the maximum load of the predicted response with that from the unreinforced experiment. This value of CTOD was used for predicting the reinforced specimen response and the subsequent parametric study. Predicted response of the unreinforced specimen was in good agreement with experiment,

American Institute of Aeronautics and Astronautics

which suggests the finite element model, material properties, and crack tip opening displacement value used to predict this response, adequately captured the important phenomena.

The reinforced specimen's response was analyzed using a similar technique except failure of the interface layer and reinforcement was included. When failure of the interface occurred the stiffness of the interface for that element was set to zero. Failure of the reinforcement was defined when the inplane stress parallel to the fiber direction exceeded the strength of the reinforcement material. When the first reinforcement element failed the symmetry constraints on the reinforcement layers along the crack path were released simulating instantaneous failure across the reinforcement. After instantaneous failure of the reinforcement, crack growth in the base aluminum layer beneath the reinforcement was progressively modeled. Crack growth was modeled past the trailing edge of the reinforcement to insure the model adequately predicted the fracture characteristics after reinforcement failure.

The analysis predicts a flattening of the response curve as the crack approaches the reinforcement as well as a slight increase in load prior to failure of the reinforcement, which compared favorably with experimental results. The slope of the response curve after the failure of the reinforcement is consistent with experimental data. Agreement between the experiment data and analysis results was considered good for this parametric study.

A second analysis of the reinforced specimen was performed, not shown here, that excluded progressive failure of the interface and only modeled crack growth to the edge of the reinforcement. Overall load-crack growth response was similar to the progressive failure case, predicting a slightly higher maximum load, and seemed to adequately capture the important internal load transfer mechanisms. Therefore, all parametric fracture studies excluded progressive interface and reinforcement failure.

Load transfer mechanisms between base aluminum and reinforcement investigated in the fatigue crack growth case are similar for the fracture cases. Three parameters investigated in this study are reinforcement width, reinforcement thickness and adhesive stiffness. As evident in the fatigue crack growth investigation, coupling between these parameters can greatly influence the magnitude of the response. The predicted results from this parametric study are presented in Figures 11 thru 16 in the form of applied load as a function of crack growth.

The effect of reinforcement width on fracture response is depicted in Figures 11 and 12. Specimens having reinforcement widths of 0.25", 0.50", and 1.0", were analyzed. These specimens were analyzed with both stiff and flexible interfaces. Maximum load and crack length at maximum load increased as a function of reinforcement width. Maximum load for the 0.50" wide reinforcement with a stiff interface increased approximately 15 percent relative to the predicted unreinforced response, as depicted in Figure 11. A similar specimen with a flexible interface, see Figure 12, exhibited approximately 8 percent increase in maximum load. In the aforementioned cases where the maximum load occurred at the edge of the reinforcement the crack length at maximum load increased by 150 percent relative to the crack length at maximum load for the unreinforced specimen. Prior to reinforcement failure, the response curve changes from a "rounded" shape (no reinforcement), to having a flattened shape with a positive slope. Increasing reinforcement width for specimens with stiff interfaces has diminishing return for widths above 0.50". The load transferred to the reinforcement with a stiff interface is reacted along the leading edge of the reinforcement with little load being reacted along the trailing edge. Therefore adding additional width has minimal affect on load transfer and hence fracture response. However, for the case of a flexible interface, additional reinforcement width results in more load transferred to the reinforcement and improved fracture response.
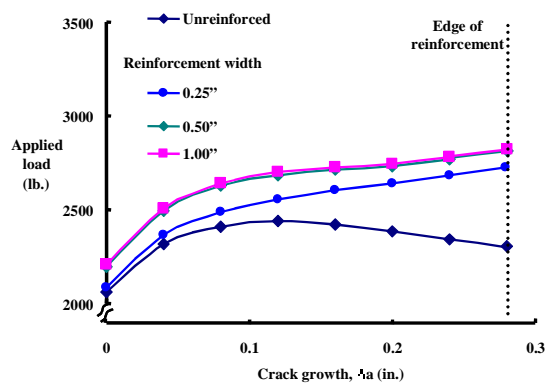

Figure 11. Predicted effect of reinforcement width on fracture response (stiff interface, reinforcement thickness = 40 percent).
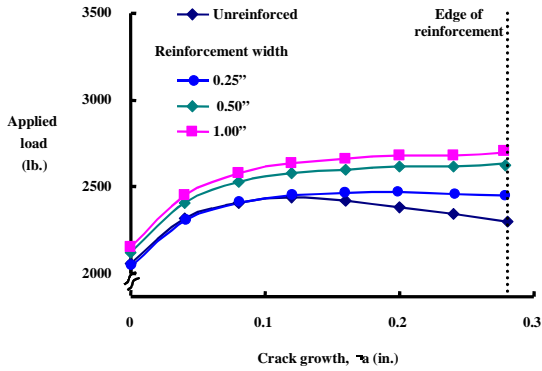
Figure 12. Predicted effect of reinforcement width on fracture response (flexible interface, reinforcement thickness = 40 percent).

Increased interface stiffness had a significant affect on the fatigue crack growth characteristics of selectively reinforced specimens due to the ability to transfer load from the base aluminum into the reinforcement over a smaller area. Similar trends are exhibited for the fracture response, as depicted in Figures 13 and 14, for specimens with reinforcement 40 percent through the thickness and widths of 0.50" and 0.25", respectively, for stiff and flexible interfaces. For the 0.50" wide reinforcement the stiff interface specimen exhibited approximately a 15 percent increase in maximum load relative to the unreinforced specimen, whereas the flexible interface specimen exhibited only an 8 percent increase in maximum load, as shown in Figure 13. For specimens with reinforcements 0.25" wide the specimen with a stiff interface exhibited an increase in maximum load of 11 percent whereas the flexible interface specimen had less than 1 percent increase in maximum load, as depicted in Figure 14.
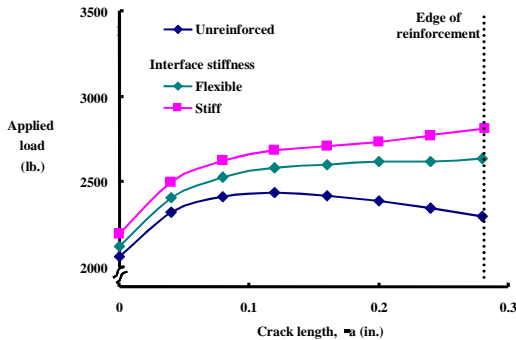

Figure 13. Predicted effect of interface stiffness on fracture response (reinforcement width = 0.50", reinforcement thickness = 40 present).
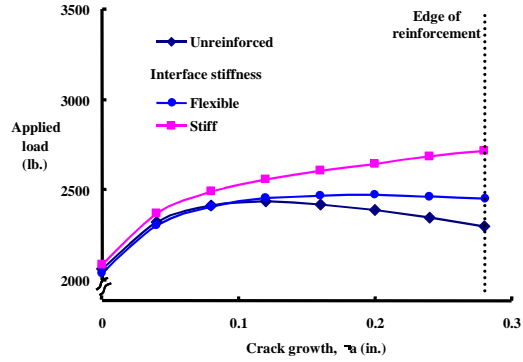

Figure 14. Predicted effect of interface stiffness on fracture response (reinforcement width = 0.25", reinforcement thickness = 40 percent).

The coupling effects of reinforcement width and interface stiffness are depicted in Figure 14 for the case of 0.25" wide reinforcement and a flexible interface. For this combination of width and interface properties the initial fracture response was essentially the same as for the unreinforced specimen. Although the maximum fracture load for this case was only slightly higher than the unreinforced specimen, the crack length at maximum load increased approximately 150 percent.

The effect of reinforcement thickness on fracture response is depicted in Figures 15 and 16. Two reinforcement thicknesses were evaluated: 40 and 80 percent through the thickness for reinforcement width of 0.50". Stiff and flexible interfaces were evaluated for these reinforcement thicknesses. As has been seen with other combinations of parameters, interface stiffness can have a dramatic affect on fracture response. For the case of the stiff interface, Figure 15, the maximum load increases with increasing reinforcement thickness. Nearly a 20 percent increase in maximum load was obtained for the specimen having an 80 percent through-the-thickness reinforcement as compared to the unreinforced specimen. The specimen having 80 percent through the thickness reinforcement achieved approximately 7 percent increase in maximum load as compared to the specimen having a reinforcement one-half as thick.
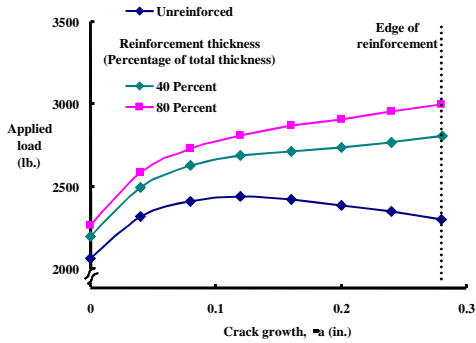
Figure 15. Predicted effect of reinforcement thickness on fracture response (reinforcement width = 0.50", stiff interface).

The results presented in Figure 16 demonstrate an important influence of interface stiffness. In this figure, results from specimens with a flexible interface are plotted. Doubling reinforcement thickness resulted in a decrease in maximum load to the extent that the reinforced specimen's response was below that of an unreinforced specimen. This is a situation where the base aluminum beneath the reinforcement accounts for only 20 percent of the total specimen thickness. Fracture response of an unreinforced specimen is a function of specimen thickness and one would expect that an unreinforced specimen that is one-fifth the thickness would have a substantially lower maximum load. Because the flexible interface does not transfer load effectively into the reinforcement, only a portion of the benefit of having reinforcement can be realized, and in this case the response is less than that of an unreinforced specimen.
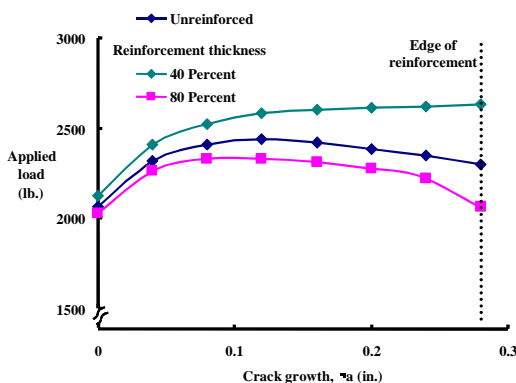

Figure 16. Predicted effect of reinforcement thickness on fracture response (reinforcement width = 0.50", flexible interface).

CONCLUSIONS

An experimental and analytical investigation of the fatigue crack growth and fracture response of aluminum-selectively-reinforced compact tension specimens was performed. It was shown that selective reinforcement had a measurable affect on both crack growth and fracture. Three important parameters that influenced this response were reinforcement width, reinforcement stiffness and interface stiffness. Based upon the cases investigated, the results depend on the extent of coupling between reinforcement geometry and material properties.

The fatigue crack growth and fracture processes were primarily affected through load sharing. In the case of fatigue crack growth, if the reinforcement reacts a sufficiently high percentage of the load then the stress-intensity factor in the base aluminum is below the stress-intensity threshold, resulting in crack arrest. In all cases when cracks arrest, the cracks extended beneath the reinforcement prior to arrest.

Fracture of selectively reinforced aluminum exhibited similar response characteristics as the fatigue crack growth process in that improvements in maximum load and crack length at maximum load were achieved through load sharing. Maximum load increased up to 20 percent for the cases investigated, whereas crack length at maximum load, for this specimen configuration; increased as much as 150 percent. Increased crack growth prior to failure provides improved opportunity to detect and repair damage prior to catastrophic failure of the structure. A further increase in maximum load is limited by the stress state in the leading edge of the reinforcement associated with the advancing crack tip.

REFERENCES

1. Farley, Gary L., "Selective Reinforcement To Enhance The Structural Performance of Metallic Compression Panels," Abstract submitted to 45th AIAA/ASME/ASCE/AHS/ASCSDM Conference, Palm Springs, CA, April 19-22, 2004.

2. "Standard Test Method for Plane-Strain Fracture Toughness of Metallic Materials," *Annual Book of ASTM Standards*, Vol. 3.01, E399, American Society for Testing and Materials, West Conshohocken, PA, 2003.

3. James, M. A. and Swenson, D. V., "A Software Framework for Two Dimensional Mixed Mode-I/II Elastic-Plastic Fracture," Mixed-Mode Crack Behavior, ASTM STP 1359, K. J. Miller and D. L. McDowell, Eds., American Society for Testing and Materials, West Conshohocken, PA, 1999.

4. Wawrzynek, P.A. and Ingraffea, A.R., "Interactive Finite element analysis of Fracture Processes: An integrated Approach," Theoretical and Applied Fracture Mechanics, No. 8, pp. 137-150, 1987.

5. Dawicke, D. S., Newman, Jr., J. C., and Bigelow, C. A., "Three-dimensional CTOA and Constraint Effects during Stable Tearing in Thin Sheet Material," ASTM STP 1256, W. G. Reuter, J. H. Underwood and J. C. Newman, Jr., Editors, American Society for Testing and Materials, Philadelphia, PA, 1995, pp. 223-242.

6. Dawicke, D. S., Sutton, M.A., Newman, Jr., J. C. and Bigelow, C. A., "Measurement and Analysis of Critical CTOA for an Aluminum Alloy Sheet," NASA TM 109024, September 1993.